

# Machine learning based algorithm for multi-FBG peak detection using generative adversarial network

SUNIL KUMAR\*, SOMNATH SENGUPTA\*

*Department of Electronics and Communication Engineering, Birla Institute of Technology, Mesra, Ranchi, Jharkhand, India*

It is suggested to use a machine learning approach based on generative adversarial networks to detect the peak wavelengths of several Fiber Bragg Gratings (FBGs). A generative model and a discriminative model make up the algorithm. The discriminative model predicts the real FBG signal by the computation of the loss functions, whereas the generative model creates a synthetic signal and is sampled for training using a deep neural network. Separate calculations are made for the loss functions of the generating and discriminative signals after training. The discriminative signal's loss function maximum and generative signal's loss function minimum are matched, and the resulting peak wavelength which is the required peak wavelength of FBG is found. Simulink in MATLAB is used to experimentally validate the suggested approach.

(Received September 7, 2022; accepted June 9, 2023)

*Keywords:* Fiber bragg grating, Generative model, Discriminative model and loss function

## 1. Introduction

An optical fibre sensor called a Fiber Bragg Grating (FBG) may be used to monitor a variety of accurate physical characteristics, including temperature, strain, torque, transmission line fault detection, humidity, magnetic field, and others [1]. The FBG can deliver highly repeatable static and dynamic sensing measurement data under any challenging circumstances. It offers greater detecting capabilities compared to conventional electronics sensors because of its compact size, longer lifespan, and lower maintenance requirements. It is more capable of resisting electromagnetic interference [2]. The FBG may therefore be used to a variety of sectors, such as aerospace [3], structure health monitoring [4], microseismic wave detection[5], inclination measurement [6], and load measuring systems [7]. An optical spectrum analyzer (OSA) is typically used to measure the reflected spectral data of FBG, however it is not appropriate for dynamic peak measurement. The experimental spectral data is recorded and stored in a computer device linked to the OSA or spectrometer using a GPIB connection, and an appropriate peak detection algorithm may be employed to determine the peak wavelength and shift in the FBG peak owing to application physical factors. There are some developed peak detection methods in this framework. Polynomial curve fitting [8], direct approach [9], centroid detection method [10], a non-linear Gaussian method [11], etc. are methods for detecting a single FBG peak. Matching filtering approach [12], Hilbert transforms [13], cross-correlation and Hilbert transform [14], Self-Adaptive [15], Invariant moment retrieval [16] etc. are techniques for multiple FBG peak identification.

The other FBG peak detection technique that is now in use was proven to work and is based on machine learning. Examples include feature extraction support

vector machine (FE-SVM)[22], deep convolutional neural network[23], decision tree with SVM[17], extreme learning machine[19], K-nearest neighbor's algorithm[20], and support vector machine (SVM)[17]. Because the FBG has a poor reflected spectrum, many of the currently available machine learning methods struggle with efficiency and mean square error during peak detection. The GAN-based machine learning approach for single FBG peak [25] is used to address these issues, however in this research, the algorithm is created for single FBG [25] and extended for multi FBG. In this study, we proposed a same Generative Adversarial Network (GAN) for multi FBGs. The proposed algorithm is verified experimentally as well as Simulink in MatLab.

## 2. Basic theory of proposed algorithm

The Fiber Bragg Grating is an optical sensor that has a reflective characteristics when the monochromatic light source pass through it. When the multiple FBGs are connected in cascaded form and broadband light source is incident then some of light ray is reflected back at wavelengths  $\lambda_{B_1}, \lambda_{B_2}, \lambda_{B_3}, \dots, \lambda_{B_n}$  for n-FBGs. The Bragg Wavelength will depends and varies with change of grating period and effective refractive index which is given as

$$\lambda_B = 2\Lambda n_{eff} \quad (1)$$

where the effective refractive index of the optical fiber's core mode is  $n_{eff}$ , the grating period is  $\Lambda$ , and the  $\lambda_B$  is the Bragg wavelength. Temperature, strain, and other

physical characteristics vary in a manner that is proportional to the change in the Bragg wavelength.

In Fig. 1, it is suggested and explained how to detect multi-FBG peak using GAN-based machine learning. The Generative Model (GM) and the Discriminative Model (DM) make up the GAN (DM). To create a synthetic signal that resembles the FBG signal in form, the GM is employed. The wavelength range of a model signal assumed in the generative model is the same as that of the FBG signal. For quick processing, a deep neural network (DNN) is used to sample and train the produced model signal. The discriminator model receives the signal from the generator model after sampling and training. To produce the genuine signal, the Discriminator model is also sampled, along with the FBG or real signal. Calculating the loss function of the real signal and created signal, the discriminative model separates the genuine signal from the synthetic signal using DNN. At a certain wavelength, which is the intended peak wavelength, the loss functions of the discriminative model are maximised and those of the generative model are minimised.

As, it is explained that the GAN model for single FBG [25] and it is extended for multi-FBG Peak detection. The GAN is combination of generative and discriminative model but both model required to train separately which is describe as

**a) Discriminator model training:**

In GAN model Discriminator model (DM) is train but the same time the other model (GM) is kept as untrained and written in eq.2, in terms of the loss function as

$$F(D_i(\lambda), G_i(\lambda)) = E(\log(D_i(\lambda))) + E(\log(1 - G_i(\lambda))) \quad (2)$$

where,  $\log(D_i(\lambda))$  is the discriminator model output as loss function and  $\log(1 - G_i(\lambda))$  is the loss function of generator.

By differentiating with regard to  $D_i(\lambda)$ , the discriminator seeks to maximise the corresponding loss

function  $F(R_i(\lambda), I(\lambda))$  in order to determine the ideal value of discriminator as

$$D^*(\lambda) = \frac{P_{R_i(\lambda)}}{P_{R_i(\lambda)} + P_{I(\lambda)}} \quad (3)$$

where,  $P_{R_i(\lambda)}$  is the probability estimation of real signal and  $P_{G_i(\lambda)}$  is the probability estimation of generated signal.

To optimize  $D_i^*(\lambda)$ , the  $P_{G_i(\lambda)}$  should be maximum and would approach to 1, the  $P_{I(\lambda)}$  is minimum at a particular point of position.

**b) Generator model training**

The Generator model train while, the discriminator model has been kept fixed and applied the process for training with the help of mathematical expression, given as,

$$F(G_i(\lambda), D_i^*(\lambda)) = E(\log(D_i(\lambda))) + E(\log(1 - D^*(\lambda))) \quad (4)$$

By combining the eq-3 and eq-4, we can write,

$$F(G_i(\lambda), D_i^*(\lambda)) = E[\log \frac{P_{R_i(\lambda)}}{P_{R_i(\lambda)} + P_{I(\lambda)}}] + E[\log \frac{P_{G_i(\lambda)}}{P_{R_i(\lambda)} + P_{I(\lambda)}}] \quad (5)$$

By using the concept of Kullback-Leibler (KL) divergence, in eq-5, the  $F(G_i(\lambda), D_i^*(\lambda))$  is minimum when the  $P_{G_i(\lambda)}$  is minimum, say equal to zero. So, the minimum of  $P_{G_i(\lambda)}$  means, the true signal is identified by calculating the loss functions of generated signal and the real FBG signal. The loss function is maximum for discriminated signal and minimum for generated signal at a specific wavelength.

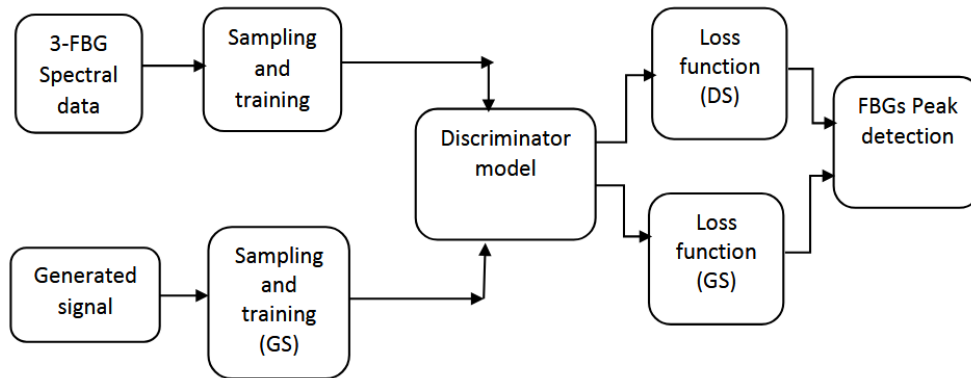


Fig. 1. Generative Adversarial network block diagram

Fig. 2 shows the proposed approach for FBG peak identification utilising a GAN training model. The relevant signal is sampled at various levels after the generative model and discriminative model are trained independently.

The levels as  $I_1, I_2, I_3, \dots, I_k$  for the produced signal and  $R_1, R_2, R_3, \dots, R_k$  for the FBG's reflectivity spectrum. The sampled data of both the

produced signal and the genuine FBG signal are moulded into discriminator levels, and the discriminator determines the true signal by computing the loss functions of both

signals. The loss function reaches its maximum for the discriminated signal and its minimum for the produced signal at the required peak wavelength.

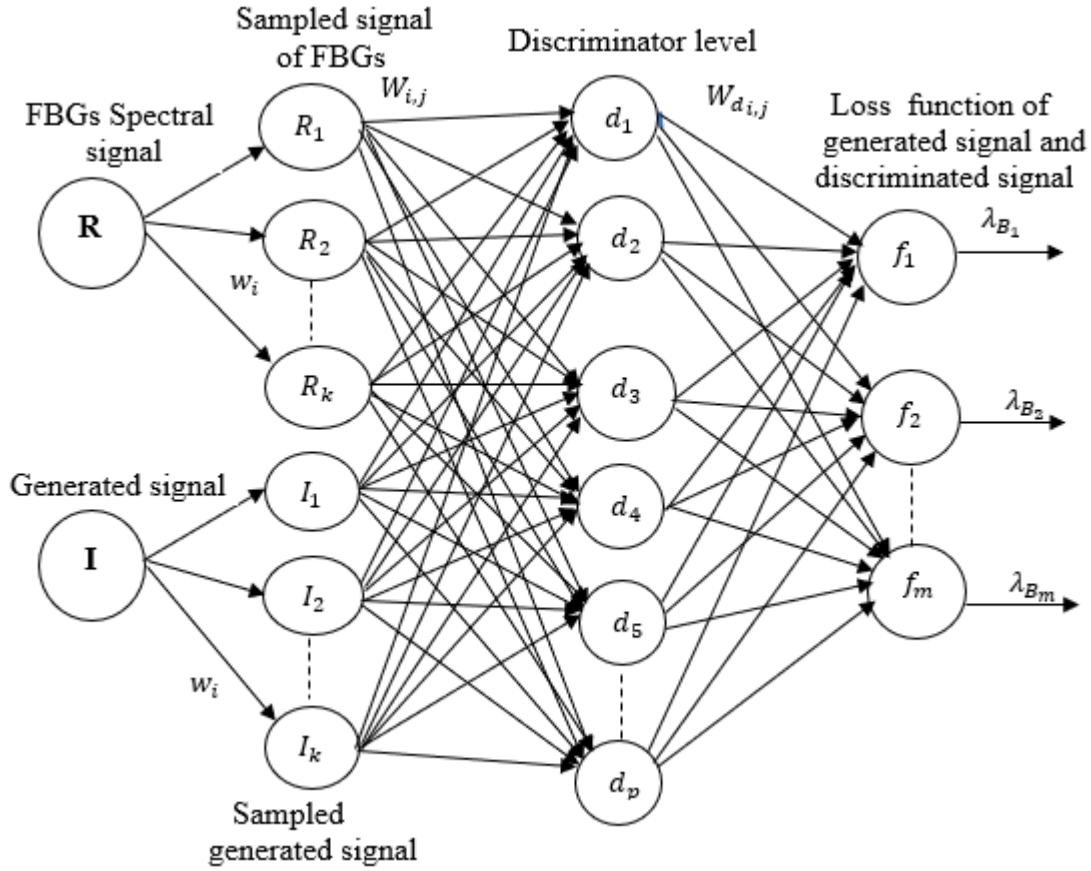


Fig. 2. DNN network structure of peak detection of FBG using GAN

$$R = \sum_{i=1}^k R_i * w_i \quad (6)$$

$$I = \sum_{i=1}^k I_i * w_i \quad (7)$$

$$\sum_{i=1}^p d_i = \sum_{i=1, j=1}^{k,p} (I_i * R_j) * W_{i,j} \quad (8)$$

$$\sum_{i=1}^m f_i = \sum_{i=1, j=1}^{p,m} d_i * W_{d,i,j} \quad (9)$$

The weight value  $W_{i,j}$  will be update until the peak of discriminated signal and generated signal matched and the

weight value  $W_{d,i,j}$  will be updated to set equipoint of minima of loss function of generated signal and maxima of loss function of discriminated signal.

### 3. Multi-FBG simulation for peak detection algorithm using GAN

Multi-FBG peak detection has been simulated utilising the suggested FBG peak detection technique employing GAN. The simulated reflected spectrum for FBGs is given as using the coupled-mode theory[24] and may be seen as

$$\sum_{i=1}^2 R_i(\lambda) = \sum_{i=1}^4 \frac{\sinh^2(\sqrt{k_i^2 - s_i^2}L)}{\cosh^2(\sqrt{k_i^2 - s_i^2}L) \frac{s_i^2}{k_i^2}} \quad (10)$$

$$k_i = \frac{2\pi}{\lambda_i} * v * dn_{eff}, \quad d_i = 2n\pi \left( \frac{1}{\lambda_i} - \frac{1}{\lambda_{B_i}} \right), \quad S_i = \frac{2\pi}{\lambda_i} * dn_{eff} \text{ and } s_i = S_i + d_i,$$

where, the  $k_i$ = ac coupling factor,  $S_i$ = dc self-coupling factor,  $d_i$ = detuning. We have considered the 2- FBG peak having wavelength range 1547 nm to 1549 nm for

FBG-1, 1549 nm to 1551 nm for FBG-2, with a central peak at 1548.14 nm, 1550.19 nm, respectively. The reflected spectrum of four FBGs are calculated and plotted in Fig. 3a. To implement the proposed peak

detection of FBGs using GAN structure, the gaussian model is used as a generator model to generate a synthetic signal having similar shape as FBGs reflected spectrum and written as.

$$I(\lambda) = he \frac{(\lambda_i - \lambda_{\tau_i})^2}{2D\lambda^2} \quad (11)$$

where, 'h' is the constant and representing the peak height of generated signal,  $D\lambda$  is the deviation in bandwidth,  $\lambda_{\tau_i}$  is the central peak of the generated signal. It is plotted in Fig. 3b. As per principle of proposed peak detection algorithm,  $\lambda_{\tau_i}$  will be varies and matched with the peak wavelength of FBGs by training of DNN. The generated signal and FBG signal are separately trained mentioned and explained in Fig. 4. The peak of FBGs spectrum and generated signal may differ after separate training of FBGs spectrum and generated signal.

The GAN based machine learning is used to reduce the problem occurs during peak matching of FBGs spectrum and synthetic signal. The regression analysis method is used for calculate the R value and plotted in Fig. 5. To analyze the regration, the deep neural network is use for training, testing and validation. The 70% of four FBGs simulated data is used for training and 30% of simulation data are used for testing. The performance of training and testing are calculates in-terms of regression (R) values as 0.99993 and 0.99993 respectively. Also, the overall performance of regression is calculated as 0.99994

and we see that, the regression value is maximum when peak of FBG spectrum and generated signal is matched. If the regression value is low then the peak are not matched. From these result we conclude that the testing and validation of proposed algorithm is performed with good accuracy. The high value of R means, the mean square error(MSE) should be very low, which is calculated as 0.0000074 at 39 epoch and plotted in Fig. 6. After 39 epoch the training, testing and validation line are cross the best set line with very less error. The performance validation low means the mean square error(MSE) is very low and nearly equal to zero. As we know, the low MSE tells the, proposed peak detection of FBG using GAN is efficiently work with good efficiency.

After regression, the loss function of discriminated signal and the loss function of generated signal are calculated and expressed as:

$$\sum_{i=1}^2 L_{g_i} = \sum_{i=1}^2 \log(1 - I(\lambda_i)) \quad (12)$$

$$\sum_{i=1}^2 L_{d_i} = \sum_{i=1}^2 \log R_i(\lambda_i) \quad (13)$$

The maxima of loss function of discriminated signal and minima of loss function of generated signal are lie on the same wavelength as 1548.14 nm, 1550.19 nm, respectively for two FBG plotted in Fig. 7. The derivative of loss function are equated with zero to find the exact peak wavelength of FBG. The simulated result is verified by experimentally in section 4.

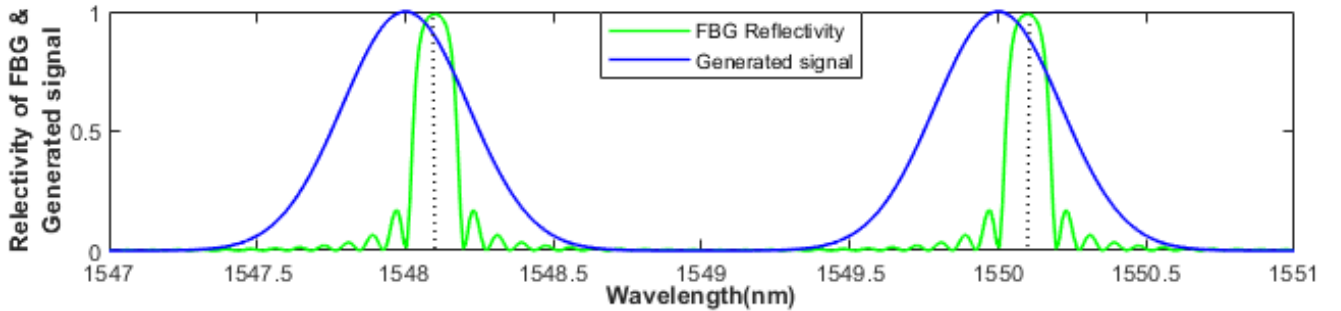


Fig. 3. Comparison response of 2-FBGs Reflectivity and generated signal (color online)

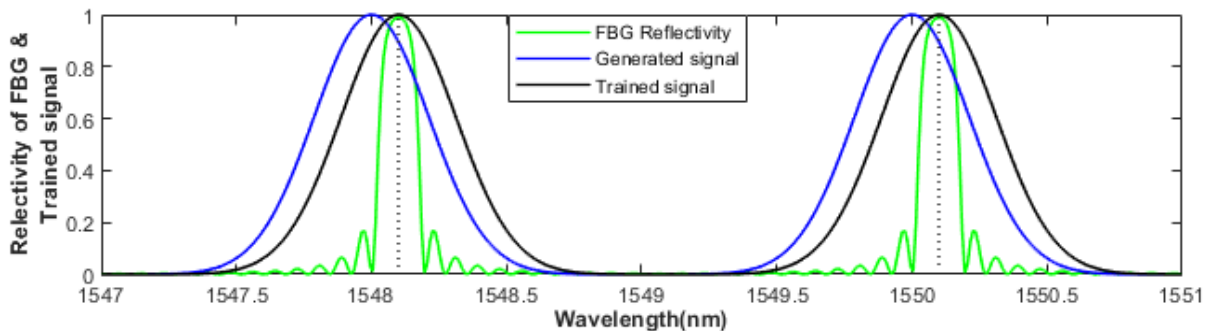


Fig. 4. Peak matching of FBGs spectrum and generated signal using DNN-GAN (color online)

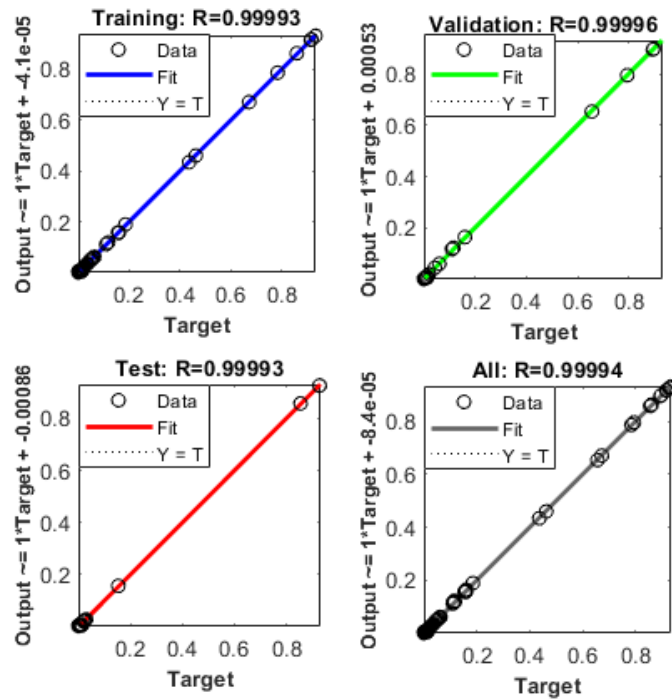


Fig. 5. Regression analysis using DNN-GAN (color online)

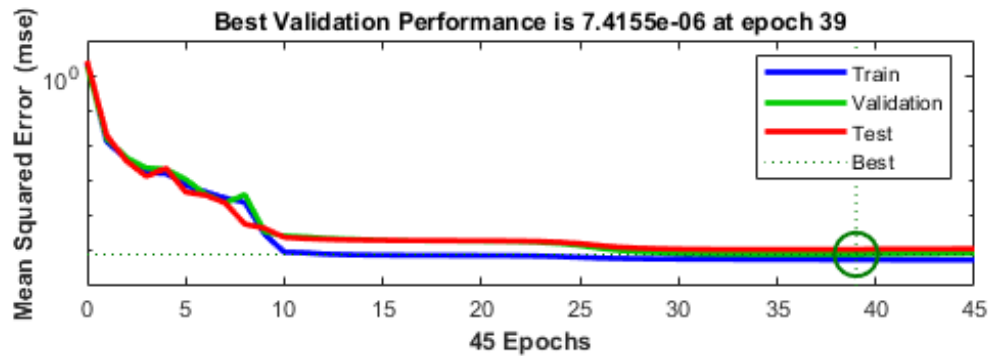


Fig. 6. Performance analysis and MSE calculation (color online)

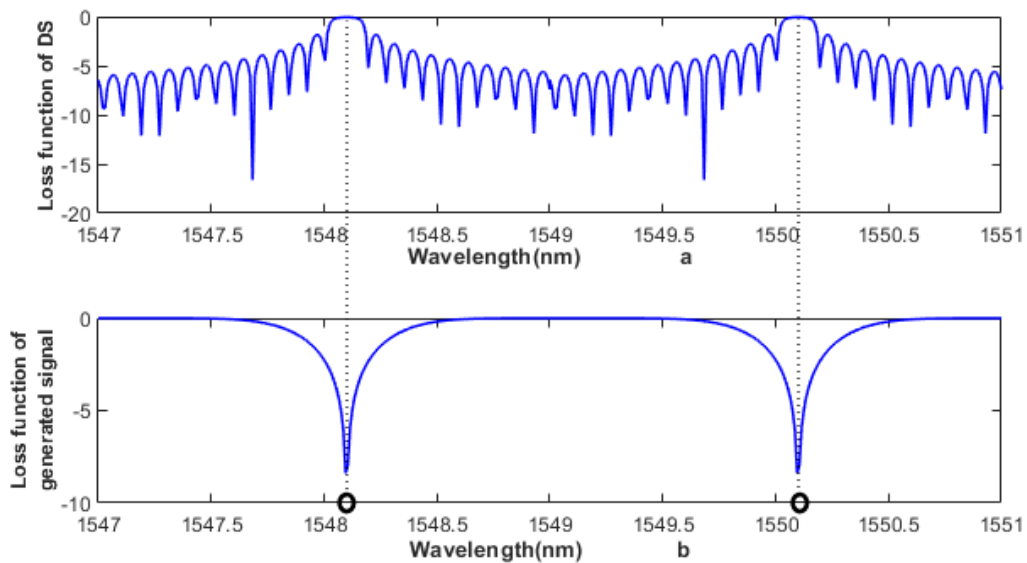


Fig. 7. Loss calculation of DM and GM and peak wavelength detection (color online)

#### 4. Experiment setup and result analysis

Experimental work is done with the suggested approach to detect multi-FBG peaks using GAN. A wideband light source is represented in the configuration in Fig. 9. (DenseLight semiconductors, DL-BX9-CS524A). Broadband light source is introduced through port 1 of Y-coupler and exits through port 2. With a wavelength range of 1547.5 nm to 1552.5 nm and a centre peak of 1549.54 nm and 1550.81 nm, respectively, the emerging light on port -2 is incident on two FBGs coupled in cascade. The FBG's reflected spectrum enters port 2 of the Y-coupler once again before exiting at port 3. A computer system that is linked to the optical spectrum analyser via GPIB cable gathers the reflected spectrum data at port-3.

Fig. 10 shows the produced signal together with the normalised spectra of two FBGs. Using a deep neural network, samples from the FBG's reflected spectrum are taken for training. The created synthetic signal is likewise sampled and trained using DNN, which is shown in Fig. 11. Regression analysis is used to examine both the produced signal and the genuine FBG signal that has been collected and trained. The training, testing, and validation features from the regression analysis are presented in Fig. 12. Also, for training, testing, and validation only, the regression value is 0.9939, 0.99207, and 0.9938, respectively. The performance of testing and validation is extremely low and very near to zero, as seen in Fig. 13. With low MSE values, a differentiated signal's loss function is at its maximum. The mu parameter, which is

$1e-7$  and has a low gradient value of 0.0022 at epoch-9, leads us to another conclusion. The performance of the min-max of the loss function of the discriminated signal and the produced signal is further validated by the training state depicted in Fig. 14. The peak of the FBG spectrum and the produced signal are matched when the regression is run, as shown in Fig. 11. We discovered this since the R-value was high. The discriminator generates the matched signal by calculating the loss function of the created signal and the real signal under consideration. At a specific wavelength, which is the intended peak wavelength, the loss function of the real signal is maximized and the loss function of the produced signal is minimized. Calculating the minima of the loss function of the produced signal and the maxima of the loss function of the distinguished genuine FBG signal yields the desired peak locations in terms of wavelength. The produced signal's minima and the discriminated signal's peak positions both lie on the same wavelength. The equipoint of both positions of the loss function is calculated as 1549.5002 nm for FBG-1 and 1550.8001 nm for FBG-2 which is plotted in Fig. 15. The measured peak wavelength is nearest to the central peak of FBG used for the experiment as 1549.5 nm for FBG-1 and 1550.8 nm for FBG-2, with a low error of 0.2 pm and 0.1 pm respectively. Hence, the proposed peak detection algorithm of Multi-FBGs using GAN is successfully performed and verified experimentally with good accuracy. Also the performance analysis of different peak detections are summarised in Table 1.

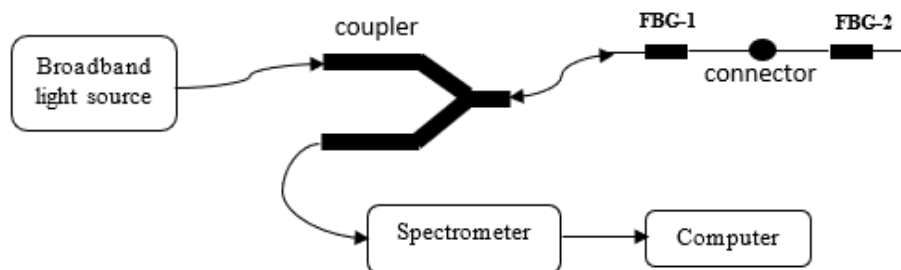


Fig. 8. Experimental setup

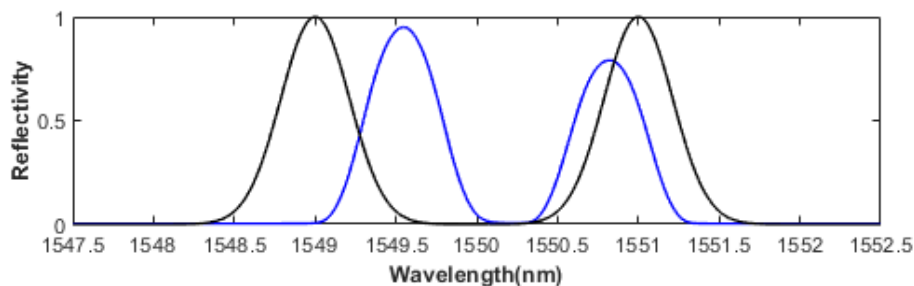


Fig. 9. Normalized experimental FBGs reflectivity and generated signal (color online)

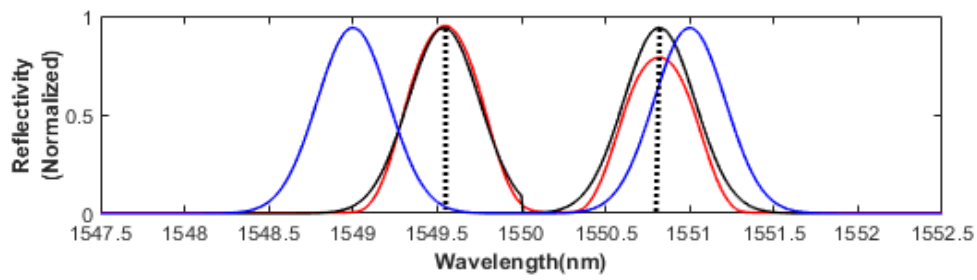


Fig. 10. Peak matching of experimental reflected spectrum of FBGs and generated signal using DNN-GAN (color online)

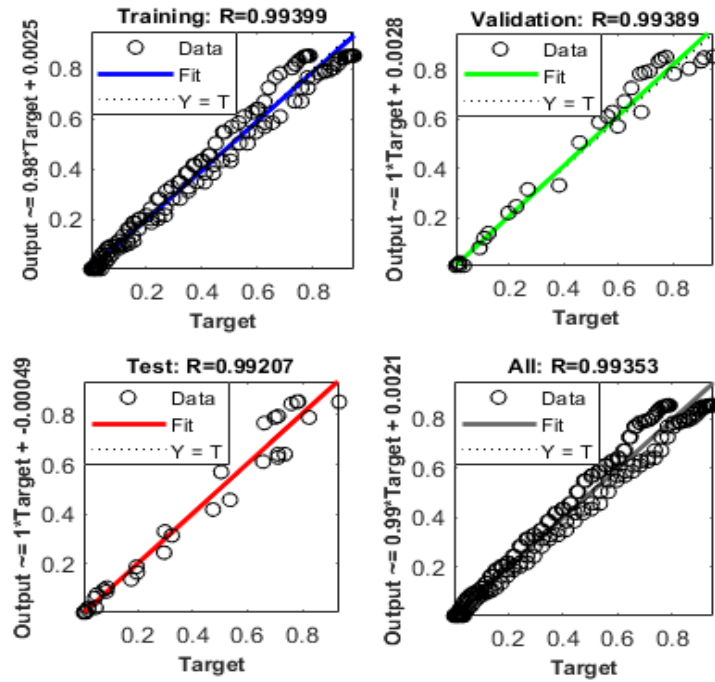


Fig. 11. Regression value calculation of experimental data (color online)

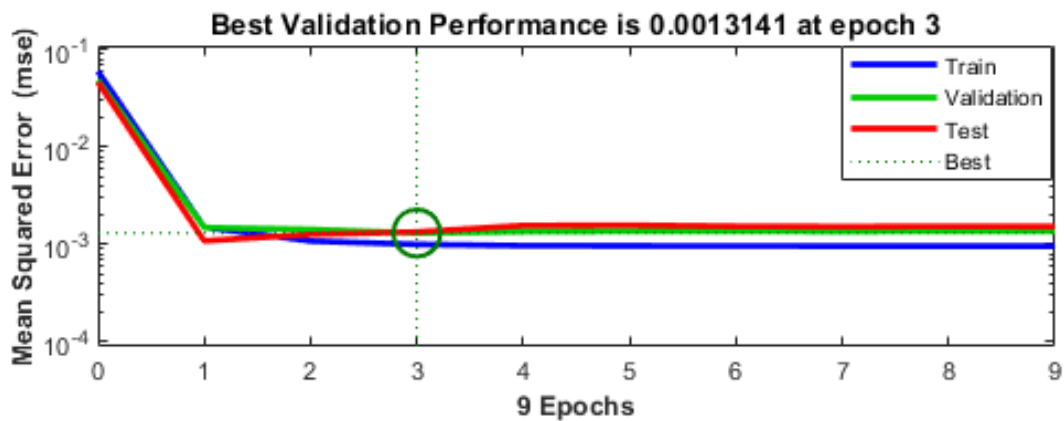


Fig. 12. Analysis of performance of DNN-GAN (color online)

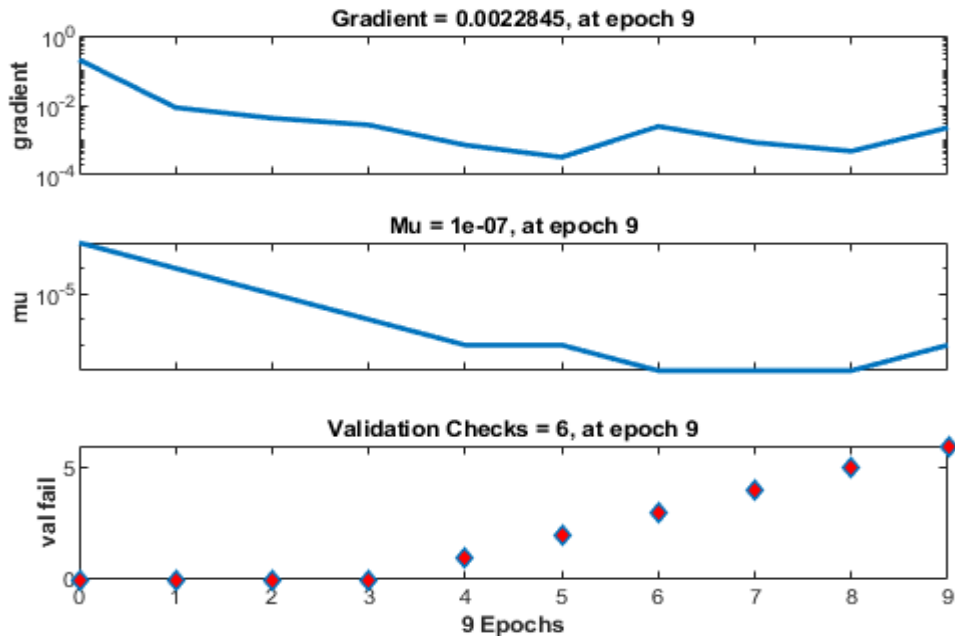


Fig. 13. Validation fail and gradient value calculation using DNN at specific epoch (color online)

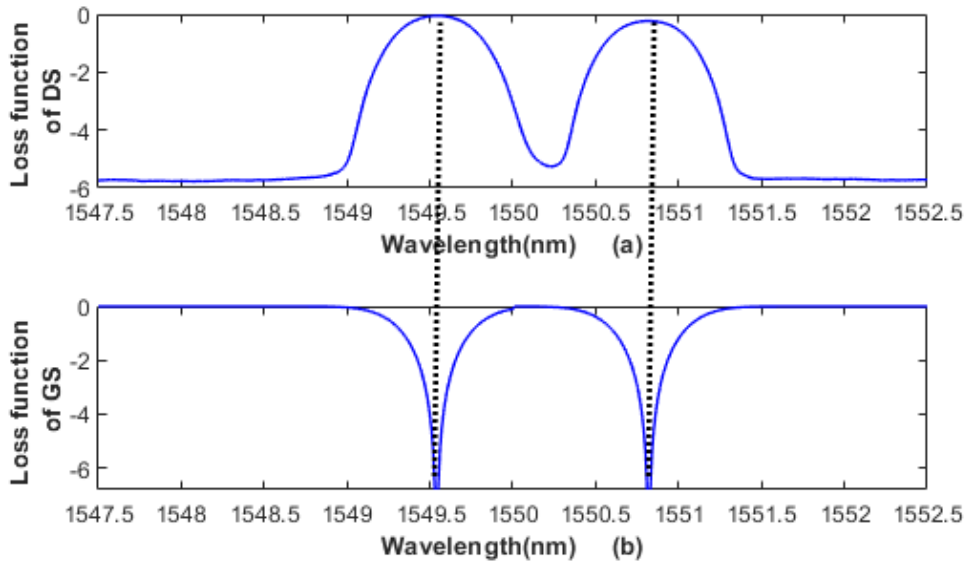


Fig. 14. Loss calculation of DM and GM and peak wavelength detection of experimental data (color online)  
 Table 1. The performance comparison of different Peak detection techniques

| Ref. no. | FGB peak detection methods based on                     | 3-dB bandwidth of the considered FBG signal | Mean     | Mean square error (MSE) |
|----------|---|---|----------|-------------------------|
| [13]     | Hilbert transform                                       | 0.212 nm                                    | 5.80 pm  | ----                    |
| [16]     | Invariants moment interval                              | 0.3 nm                                      | 0.19 pm  | 0.5 pm                  |
| [18]     | Machine learning techniques for liquid level estimation | 0.5 nm                                      | ----     | 3.58 cm                 |
| [19]     | E-machine learning                                      | ----  | ----     | 0.918 pm                |
| [26]     | GAN-DNN based Machine learning                          |   |          | 3 pm                    |
| -----    | GAN (present work)                                      | 0.3 nm                                      | 0.008 pm | 0.20 pm                 |



## 5. Conclusions

The proposed peak detection algorithm of FBG using Generative Adversarial Network (GAN) is successfully developed. The algorithm is verified by experimental and simulation in MATLAB. Basically, GAN is based on Generative and Discriminative model. A random gaussian signal is generated by generative model and sampled for mixing the signal with real FBG signal for discriminating the real signal by discriminator. The loss function is calculated of generated signal and discriminated signal when the peak of generated signal is matched with real signal after training separately at least 1 or 2 epochs. The peak wavelength is calculated as 1549.5002 nm for FBG-1 and 1550.8001 nm for FBG-2. Also, the error is calculated as 0.2 pm and 0.1 pm respectively with MSE as 0.0022. The performance of regression analysis is measured as 0.9935, hence, the multi-FBG peak detection using GAN is performed with high efficiency and good accuracy. The future work is to perform the same algorithm in time domain.

## References

- [1] G. Y. Chen, G. Brambilla, Optical Fiber Sensors, CRC Press, 2017.
- [2] Shizhuo Yin, Paul B. Ruffin, Francis T. S. Yu, Fiber Optic Sensors, CRC Press, 435 (2008).
- [3] Z. Ma, X. Chen, Sensors **19**(1), 55 (2018).
- [4] Sagar Jinachandran, Hui Jun Li, Jiangtao Li, Gangadhara B. Prusty, Yuliya Semenova, Gerald Farrell, Ginu Rajan, IEEE Sensors Journal **18**(21), 8739 (2018).
- [5] Abhinav Gautam, Amitesh Kumar, Vishnu Priye, Optical Engineering **58**(5), 056111 (2019).
- [6] Kumar Kinjalk, Amitesh Kumar, Abhinav Gautam, IEEE Transactions on Instrumentation and measurement **69**(11), 9124 (2020).
- [7] Neil J. Vickers, Current biology **27**(14), R713 (2017).
- [8] Y. An, X. Wang, Z. Qu, T. Liao, Z. Nan, Optik **172**, 753 (2018).
- [9] Z.-J. Chen, J. Bai, Z.-T. Wu, X.-H. Zhao, J.-J. Zhang, Acta Photonica Sinica **44**(11), 1112001 (2015).
- [10] A. Trita, E. Voet, J. Vermeiren, D. Delbeke, P. Dumon, S. Pathak, D. van Thourhout, IEEE Photonics Journal **7**(6), 11 (2015).
- [11] Junfeng Jiang, Yining Yang, Xuezhi Zhang, Kun Liu, Shuang Wang, Xiaojun Fan, Fang Sun, Hai Xiao, Tiegeng Liu, Optical Fiber Technology **45**, 399 (2018).
- [12] Sunil Kumar, S. Sengupta, Optical and Quantum Electronics **54**(2), 1 (2022).
- [13] Liu, Fang, Xinglin Tong, Cui Zhang, Chengwei Deng, Qiao Xiong, Zhiyuan Zheng, Pengfei Wang, Optical Fiber Technology **45**, 47 (2018).
- [14] A. Theodosiou, M. Komodromos, K. Kalli, Journal of Lightwave Technology **35**(18), 3956 (2017).
- [15] Y. Chen, K. Yang, H.-L. Liu, IEEE Sensors Journal **16**(8), 2658 (2016).
- [16] Y. Guo, C. Yu, Y. Ni, H. Wu, Optical Fiber Technology **54**, 102129 (2020).
- [17] H. Li, K. Li, F. Meng, X. Lou, L. Zhu, Optical Fiber Technology **60**, 102371 (2020).
- [18] K. Pereira Nascimento, A. Frizera-Neto, C. Marques, A. G. Leal-Junior, Optical Fiber Technology **65**, 102612 (2021).
- [19] H. Jiang, J. Chen, T. Liu, IEEE Photonics Technology Letters **26**(20), 2031 (2014).
- [20] A. G. Leal-Junior, V. Campos, C. Diaz, R. M. Andrade, A. Frizera, C. Marques, Optical Fiber Technology **56**, 102184 (2020).
- [21] Yen-Jie Ee, Kok-Soon Tey, Kok-Sing Lim, Prashant Shrivastava, S. B. R. S. Adnan, Harith Ahmad, Journal of Energy Storage **40**, 102704 (2021).
- [22] H. Li, K. Li, H. Li, F. Meng, X. Lou, L. Zhu, Optical Fiber Technology **60**, 102371 (2020).
- [23] Z. Cao, S. Zhang, T. Xia, Z. Liu, Z. Li, Journal of Lightwave Technology **40**(13), 4429 (2022).
- [24] Y. Guo, C. Yu, Y. Ni, H. Wu, Optical Fiber Technology **54**, 102129 (2020).
- [25] S. Kumar, S. Sengupta, Opto-Electronics Review **30**, e144227 (2022).
- [26] S. Li, S. Ren, S. Chen, B. Yu, Applied Sciences **12**(18), 9031 (2022).

\*Corresponding authors: skp.narayan@gmail.com;  
ssengupta@bitmesra.ac.in